Remotely nano-rupturable yolk/shell capsules for magnetically-triggered drug release†

Shang-Hsiu Hu,[a] You-Yin Chen,[b] Ta-Chung Liu,[a] Tsan-Hua Tung,[a] Dean-Mo Liu*[a] and San-Yuan Chen*[a]

Received 21st September 2010, Accepted 16th November 2010
DOI: 10.1039/c0cc03998e

Yolk/shell capsules containing a volume/hydrophobicity transformable core and an ultra-thin silica shell have been prepared. When an external magnetic field induced the temperature, the cores exhibit a significant triggering size shrinkage and the diameter decreases more than 10 times, causing solid shells destruction and physical collapse, leading to drug burst release.

Biocompatible yolk/shell capsules are hollow colloidal particles that can be remotely triggered release, making them attractive for their potential applications in drug delivery because the dense shells of these capsules provide both chemical and physical shielding from the surrounding environment, which can reduce undesired drug release.[1] Yolk/shell structures also have a cavity that allows for efficient delivery of proteins and nucleic acids.[2] Furthermore, the interior of these particles can be functionalized by encapsulating guest species, allowing them to be tuned to obtain a variety of desired properties.[3] Burst drug release *via* physical rupture exhibits several advantages; for example, drug molecules are not covalently bound to the drug carriers avoiding the need to alter the molecule's original properties and for chemical treatment to cleave bonds. However, to the best of our knowledge, the synthesis of yolk/shell capsules possessing a cavity and their application for remotely triggered drug release has not yet been studied.

Many studies have reported controlled drug release systems with material responses to stimuli including temperature,[4] pH,[5] and ultrasound.[6] Recently, functional nanomaterials have widely been used as energy-induced media to trigger drug release for cancer therapy.[7] For example, the photothermal effects of gold nanostructures, nanocages and carbon nanotubes can be activated by irradiation with near-infrared (NIR) light for tumor therapy.[8] A high frequency magnetic field or NIR can cause an increase in the temperature of magnetic nanoparticles, which could be a tool useful for creating local hyperthermia and as an approach to cancer therapy. However, such a high temperature is not suitable for treatment of non-cancerous tissues or for normal drug release because the heat will likely kill healthy cells and destroy the activities of drug molecules. This activity would be a particular problem when delivering biomolecules like proteins. To address this technical challenge, we reported a simple and versatile synthetic approach that can achieve a magnetically-triggered drug release at a low temperature. Here, we have designed and fabricated yolk/shell capsules containing a magnetic core composed of iron oxide nanoparticles, a thermally responsive PEO–PPO–PEO polymer (poly(ethylene oxide)–poly(propylene oxide)–poly (ethylene oxide), known as Pluronic),[9] and an ultra-thin silica shell for efficiently regulating the drug release behavior before and after the magnetic trigger. The integration of these functions is critical for the development of a novel yolk/shell capsule that can be broadly applied as a drug and protein delivery vehicle for biomedical applications. These capsules would not only protect the drug molecules before release, but would also enable magnetically-triggered drug release at a well-tolerated temperature.

Fig. 1a presents a schematic illustration of the synthetic procedure that was used to synthesize the yolk/shell capsules. The first step involved mixing the iron oxide nanoparticles and the hydrophobic drug in an organic solvent to form a uniform phase. Next, the mini-emulsion method was applied using

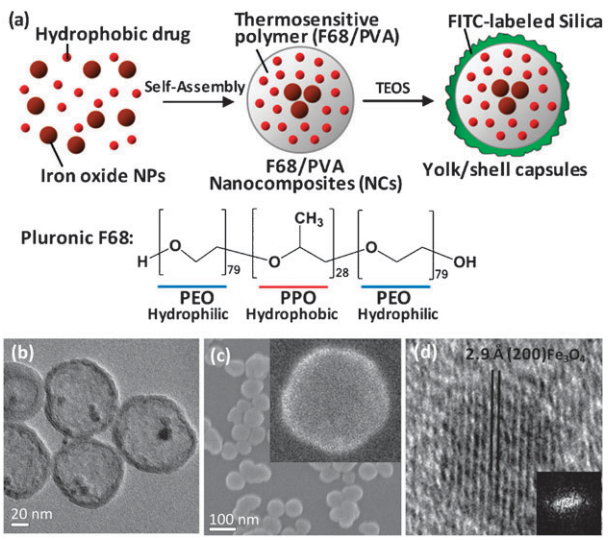

Fig. 1 (a) Schematic illustration of the synthesis and structure of the nano-rupturable yolk/shell capsules for magnetically-triggered controlled drug release. TEM images of (b) yolk/shell-1. (c) SEM image of the yolk/shell capsules. (Inset picture: higher magnification of SEM image.) (d) TEM image of lattice structure of iron oxide nanoparticles in the capsules. The yolk/shell capsules with an average diameter of about 76 nm possessed an ultra-thin layer of dense silica shell of about 7 nm in thickness.

[a] *Department of Materials Sciences and Engineering, National Chiao Tung University, Hsinchu, 300, Taiwan. E-mail: sanyuanchen@mail.nctu.edu.tw, deanmo_liu@yahoo.ca*
[b] *Institute of Biomedical Engineering, National Yang-Ming University, Taipei, Taiwan*

† Electronic supplementary information (ESI) available: Experimental procedures, characterization methods, Fig. S1–S4, and Table S1 and S2. See DOI: 10.1039/c0cc03998e

blended polymers, polyvinyl alcohol (PVA) and pluronic F68 as a binder to fabricate the self-assembling nanocomposites (NCs).[10] Because PVA and pluronic F68 are amphiphilic polymers, the hydrophobic segments of these polymers generated the driving force for the formation of iron oxide nanoparticles. While the organic solvent gradually evaporated, the polymers encapsulated the iron oxide nanoparticles and the hydrophobic drug within the composite. This encapsulation is believed to result from non-covalent interactions between the functional groups on the iron oxide surface and the hydroxyl groups of the PVA and F68. These groups may interact through hydrogen bonds or dipole–dipole interactions, resulting in an amphiphilic, polymer-induced structural self-assembly. Following this, the NCs were coated with a thin layer of silica by hydrolysis and condensation of TEOS to obtain the final yolk/shell capsules.[11] Different ratios of PVA/F68 and iron oxide nanoparticles were used in this system as shown in Table S1 (ESI†) to examine the effects of composition on thermosensitivity. Fig. 1b presents a TEM image of the resulting yolk/shell capsules. These capsules had an average diameter of approximately 76 nm and possessed an ultra-thin layer of dense silica, forming a shell approximately 7 nm in thickness. No observable crevices or cracks were detectable microscopically in the regions between the core structure and the silica shell, suggesting a compatible interface between these two materials. Furthermore, as shown in the TEM image, there were only 2–5 iron oxide nanoparticles per capsule, and the polymer matrix accounted for a large portion of the capsule volume, providing sufficient space for drug loading. The scanning electron microscopy (SEM) image of the resulting yolk/silica shell capsules shown in Fig. 1c reveals the surface structure and morphologies of the capsules. The silica shells did not display any crevices or cracks in the SEM image, indicating that the core had a dense and continuous structure. In the HR-TEM image shown in Fig. 1d, the magnetic phase (Fe_3O_4) can be clearly identified as a crystalline structure. Yolk/shell capsules with increasing F68/PVA ratios exhibited similar structures as seen in Fig. S1 (ESI†). Silica shells approximately 7–10 nm in thickness still covered the Fe_3O_4/polymer core/shell nanocomposites (NCs).

In Fig. 2a, the release patterns from the yolk/shell capsules are predominantly regulated by the silica shells. In these systems, the rate of release is relatively slow, reaching only 6% over 48 h. This finding clearly indicates that the inorganic silica shell, although it is only 5 nm thick, acts as an effective barrier to block the drug molecules from passive diffusion due to its density and stability. The thermosensitivity of these yolk/shell capsules is based on PEO–PPO–PEO triblock polymers that manifest a range of critical micelle temperatures (CMT) for volume/hydrophobicity transitions, meaning that the inter-chain aggregation of PEO–PPO–PEO triblock copolymers above CMT forms alternating PEO and PPO layers into micelles, causing a volumetric transition due to the water solubilization/rejection in the PPO domain.[12] The capsule cores display thermosensitive behavior similar to that of the PEO–PPO–PEO polymer, including shrinkage above the CMT. The sizes of capsules without silica shells, *i.e.*, F68/PVA nanocomposites (NCs), were measured by DLS at different temperatures. Fig. 2b shows the size of F68/PVA NCs as a

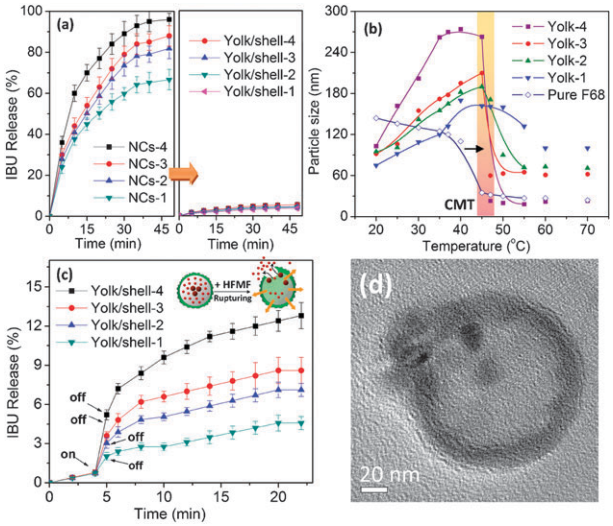

Fig. 2 (a) Cumulative drug release of F68/PVA nanospheres (yolk) and yolk/shell capsules ($n = 3$). (b) Diameter of F68/PVA nanospheres measured by DLS decreased abruptly at about critical micellization temperature (CMT). (c) Cumulative drug release profiles of ibuprofen (IBU) from yolk/shell capsules were triggered by a high frequency magnetic field (HFMF) for 1 minute at the fourth minute ($n = 3$). (d) After the exposure to a magnetic field, the volume/hydrophobicity transition of cores produced a strong inner stress, making the capsules rupture as demonstrated in TEM image.

function of temperature, where a transition is revealed by the large change in size between 45 °C and 50 °C. The CMT of the F68/PVA series (47 °C) is higher than that of pure F68 (43 °C) because PVA introduces more hydrophilic functional groups to the nanostructures, resulting in stronger interactions such as hydrogen bonding between the PVA and F68.

The size ratio is defined as d_{max}/d_{min}, where d_{max} is the maximum particle diameter below the CMT at the lowest temperature and d_{min} is the minimum particle diameter above the CMT at the highest measured temperature. The d_{max}/d_{min} for NCs with a F68 : PVA ratio of 10 : 5 is 11, much higher than the d_{max}/d_{min} ratio seen when the F68 : PVA ratio is 1 : 5 ($d_{max}/d_{min} = 1.8$). This finding indicates the obvious shrinking that occurs once the temperature has crossed the CMT threshold, as shown in Fig. 2b. Both the hydrophilic "swollen" state and the hydrophobic "shrunken" state appear to be constrained by the presence of PVA. NCs with PVA displayed larger volume/hydrophobicity transition properties than pure F68 nanospheres.

Fig. 2c shows the IBU release profiles from yolk/shell capsules under magnetic fields of 2.5 kA m^{-1} at a frequency of 50 kHz. For the magnetically triggered drug-release system, the heat induced by the magnetic field triggers drug release. Heat generation, governed by the mechanism of magnetic energy dissipation for single-domain particles (Brown and Néel relaxations), has been well documented. A significant acceleration in release was observed in the fourth minute of subjection to the magnetic field, which was not seen in the absence of the magnetic stimulus. With higher ratios of the thermosensitive polymer, the controlled release from yolk/shell capsules increased to 5.3% within 1 min of exposure to the stimulus. The release profile of the yolk/shell capsules was not

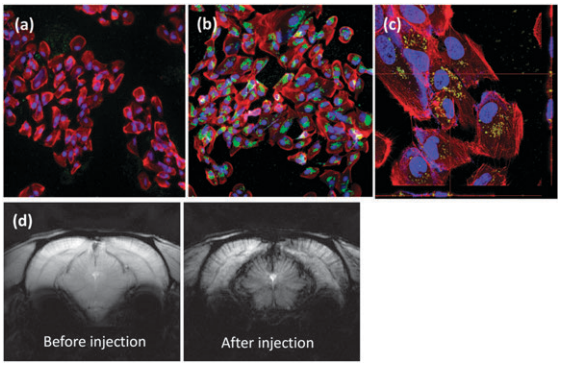

Fig. 3 Time-course confocal images of ARPE-19 cells incubated with FITC-labeled yolk/shell capsules (green dots) for (a) 4 and (b) 24 hours. The cells were stained with rhodamine phalloidin (red), and cell nucleus with DAPI (blue). (c) The cross section images of cells viewed by a laser-scanning confocal microscope. (d) MR images of rat brain before and after the intravenous injection of yolk/shell capsules. Image was acquired pre-injection (left) and 2 h post-injection (right).

restored right after the removal of the stimulus, and the release rate was considerably increased compared to that of the as-prepared yolk/shell capsules that were not subjected to any magnetic field treatment. This finding suggests that the nanostructures were physically and irreversibly deformed, thus maintaining their rapid release rate after removal of the stimulus. After a short exposure to the stimulus (60 s), in TEM image of Fig. 2d, the silica shell of the capsules was deformed as a result of rapid shrinkage of the core phase, causing irreversible cracks in the silica shells. Thermosensitive cores showed a dramatic change in size and enlarged nano-scale crevices after magnetic heating, which permitted dye molecules to easily escape from the capsule and ultimately formed a severe crack and led to the irreversible deformation or rupture of the shell.

Cellular uptake of the FITC-labeled yolk/shell capsules was investigated using confocal microscopy. This study used a normal cell model of retinal pigment epithelium (RPE) cells (ARPE-19), which are from a monolayer of hexagonal cells separating the neural retina from the underlying choroidal vascular bed. In Fig. 3a, for the 4 hour incubation, some of the capsules appeared as green dots that were attached to the surface of the cell membranes; however, most of the capsules were still dispersed on the plate. Increasing the uptake time to 24 hours, shown in Fig. 3b, resulted in a greater adsorption of the FITC-labeled capsules onto the cells, and some capsules also appeared to reside inside the cells. The cross-section of the confocal images in Fig. 3c demonstrates considerable regions of the cytoplasm displaying strong green fluorescence, suggesting that the capsules are efficiently localized within the cell.

The small effect of the capsules on cell viability led us to study the capsules *in vivo* as MR imaging agents as shown in Fig. 3d. Healthy rats were intravenously injected with yolk/shell capsules (12 mg kg^{-1}, 0.3 mL). Injection of the capsules enhanced the image contrast of MR images of rat brains and enabled the visualization of blood vessels, indicating that these yolk/shell capsules can serve as MRI contrast agents as well as drug delivery vehicles. These yolk/shell capsules provide an avenue for controlled drug delivery and offer a potential advantage for bioimaging and biomedical applications requiring drug release following physical rupture caused by external application of a magnetic field.

In summary, yolk/shell capsules have been prepared with a soft thermosensitive core and a thin but dense silica shell. The yolk/shell capsules can be triggered burst release by an external magnetic field through the hydrophilic-to-hydrophobic transition of an inner polymer at a characteristic temperature (CMT) that triggers a size contraction as large as 10 fold, leading to the capsule physical rupture. These capsules were also efficiently taken up by healthy cell lines and can be used as MR contrast agents. Future development of this new class of functional yolk/shell capsules includes targeted imaging and therapy *in vitro* and *in vivo*, and we envision that this enabling technology will open exciting opportunities in nanomedicine and biotechnology.

Notes and references

1 A. Corma, U. Díaz, M. Arrica, E. Fernández and Í. Ortega, *Angew. Chem., Int. Ed.*, 2009, **48**, 6247.
2 (*a*) Y. Lu, Y. Zhao, L. Yu, L. Dong, C. Shi, M. J. Hu, Y. J. Xu, L. P. Wen and S. H. Yu, *Adv. Mater.*, 2010, **22**, 1407; (*b*) Y. Yin, R. M. Rioux, C. K. Erdonmez, S. Hughes, G. A. Somorjai and A. P. Alivisatos, *Science*, 2004, **304**, 711; (*c*) Y. Sun and Y. Xia, *Science*, 2002, **298**, 2176.
3 (*a*) X. J. Xu and D. Xu, *J. Am. Chem. Soc.*, 2009, **131**, 2774; (*b*) Y. S. Lin, S. H. Wu, C. T. Tseng, Y. Hung, C. Chang and C. Y. Mou, *Chem. Commun.*, 2009, 3542.
4 Z. Ge, J. Hu, F. Huang and S. Liu, *Angew. Chem., Int. Ed.*, 2009, **48**, 1798.
5 M. S. Kim and D. S. Lee, *Chem. Commun.*, 2010, **46**, 4481.
6 (*a*) H. J. Kim, H. Matsuda, H. Zhou and I. Honma, *Adv. Mater.*, 2006, **18**, 3083; (*b*) B. G. De Geest, A. G. Skirtach, A. A. Mamedov, A. A. Antipov, N. A. Kotov, S. C. De Smedt and G. B. Sukhorukov, *Small*, 2007, **3**, 804.
7 (*a*) X. An, F. Zhang, Y. Zhu and W. Shen, *Chem. Commun.*, 2010, **46**, 7202; (*b*) J. Lee, J. Yang, H. Ko, S. J. Oh, J. Kang, J. H. Son, K. Lee, S. W. Lee, H. G. Yoon, J. S. Suh, Y. M. Huh and S. Haam, *Adv. Funct. Mater.*, 2008, **18**, 258.
8 (*a*) J. Yang, J. Lee, J. Kang, S. J. Oh, H. J. Ko, J. H. Son, K. Lee, J. S. Suh, Y. M. Huh and S. Haam, *Adv. Mater.*, 2009, **21**, 4339; (*b*) M. S. Yavuz, Y. Cheng, J. Chen, C. M. Cobley, Q. Zhang, M. Rycenga, J. Xie, C. Kim, K. H. Song, A. G. Schwartz, L. V. Wang and Y. Xia, *Nat. Mater.*, 2009, **8**, 935.
9 S. H. Choi, J. H. Lee, S. M. Choi and T. G. Park, *Langmuir*, 2006, **22**, 1758.
10 K. Landfester, *Angew. Chem., Int. Ed.*, 2010, **48**, 4488.
11 S. H. Hu, D. M. Liu, W. L. Tung, C. F. Liao and S. Y. Chen, *Adv. Funct. Mater.*, 2008, **18**, 2946.
12 (*a*) T. Y. Liu, K. H. Liu, D. M. Liu, S. Y. Chen and I. W. Chen, *Adv. Funct. Mater.*, 2009, **19**, 616; (*b*) T. Y Liu, S. H. Hu, D. M. Liu, S. Y. Chen and I. W. Chen, *Nano Today*, 2009, **4**, 52.

